ELSEVIER

Journal of Power Sources 86 (2000) 417–422

JOURNAL OF POWER SOURCES

www.elsevier.com/locate/jpowsour

Influence of citrate–nitrate reaction mixture packing on ceramic powder properties

Klementina Zupan [a,*], Drago Kolar [b], Marjan Marinšek [a]

[a] *Faculty of Chemistry and Chemical Technology, University of Ljubljana, Aškerčeva 5, 1000 Ljubljana, Slovenia*
[b] *Jožef Stefan Institute, University of Ljubljana, Jamova 39, 1000 Ljubljana, Slovenia*

Received 5 October 1999

Abstract

Lanthanum chromite-based materials have a good prospect for use in various high temperature applications, as well as an SOFC separator. A citrate–nitrate gel combustion reaction was used for the preparation of submicron crystalline strontium-substituted lanthanum chromite (LSC). The effect of the fuel-oxidant molar ratio and sample form prior to combustion was investigated in terms of reaction period, phase formation, particle size, morphology and agglomerate formation. Several characterization methods including scanning electron microscopy, mercury porosimetry, BET measurement, X-ray powder diffraction and thermal analysis were used to evaluate the influence of reaction mixture packing on powder characteristics for different citrate–nitrate (c/n) ratios. It was shown that the reaction period depends on the fuel/oxidant ratio and reaction mixture packing. The LSC powders prepared via the combustion route exhibited surface areas of about 12 m^2/g for the loose packed layer prepared samples and 7 to 11 m^2/g for samples prepared from a pellet. The nature of the agglomerates was studied from the pore size distribution in the green compacts pressed at different pressures. The sintering behaviour of powders and some of the electrical properties of sintered samples are reported. Sintering tests on LSC powders prepared via the combustion route showed that the sintering process started at about 900°C and proceeded in two steps in the presence of a liquid phase.

Keywords: Citrate; Nitrate; Lanthanum chromite; Ceramic powder

1. Introduction

Lanthanum chromite is of interest use as material for high temperature applications, including the interconnect in solid oxide fuel cells and electronic conductors for heating elements, due to its chemical stability at elevated temperatures and electrical properties. However, lanthanum chromite-based materials are difficult to fabricate into a dense gas-tight separator between the electrodes. The most significant influence on their densification can be achieved by substitution of alkaline earth elements (Mg, Ca, Sr) for a fraction of *A* or *B* lattice sites in the perovskite structure, and also by using fine reactive powder [1]. Doping elements decrease evaporation of chromium oxide or form a liquid phase with chromite during sintering, and influence electrical conductivity as well [2]. Some difficulties with the interconnect formation can be diminished if the powder particles are small (<1 μ). Good sinterability may be achieved when nonagglomerated powders are employed or the preparation procedure is such that weak agglomerates are formed. Hard and dense agglomerates in ceramic powders usually result in large interagglomerate pores after sintering [3].

Preparation of complex metal oxides is traditionally carried out by solid state synthesis, i.e., the ''calcining'' method. Several synthetic techniques are available for the preparation of multicomponent oxides, e.g., the solid-solution-precursor method [4], sol–gel synthesis [5], co-precipitation [6], and spray drying [16]. Each method has its own characteristic compositional homogeneity, powder morphology and degree of agglomeration. Combustion synthesis is also an important and promising powder preparative technique due to its low energy and time consumption. The critical factors of combustion synthesis are the fuel/oxidant ratio and sample packing prior to ignition; these determine the temperature and reaction time, control the

* Corresponding author.

0378-7753/00/$ - see front matter
PII: S0378-7753(99)00406-1

degree of conversion, phase formation, particle morphology and the nature of the agglomerates. The exothermic effect during fuel and nitrate decomposition is accompanied by a large gas release that prevents hard agglomerate formation. Combustion synthesis that employs some explosive mixtures such as nitrates with urea or glycine normally requires specialized apparatus and only small amounts of the product can be prepared. The citrate–nitrate gel combustion reactions are more controllable due to their much less severe exothermic reactions, allowing preparation of larger amounts of the product.

In the present contribution for the different fuel oxidant ratios, we describe the influence of sample form prior to combustion on the reaction period, powder characteristics, phase formation and degree of conversion for strontium substituted lanthanum chromite prepared by citrate–nitrate gel combustion synthesis. Roy et al. [7] derived the applied method from the citrate-gel precursor synthesis [8].

2. Experimental method

Samples with nominal composition $La_{0.7}Sr_{0.3}CrO_3$ (LSC) were prepared by combustion synthesis of citrate–nitrate gel. In the combustion method, the starting materials (analytical reagent grade) were $La(NO_3)_3 \cdot 9H_2O$, $Cr(NO_3)_3 \cdot 6H_2O$ and $Sr(NO_3)_2$. They were mixed in an appropriate molar ratio, dissolved in a minimum quantity of water and 2.9 M citric acid solution was added. The citrate–nitrate (c/n) ratios in the reaction mixtures were 0.28, 0.23 and 0.18. The dish was kept over a water bath at 60°C under vacuum (20 mm Hg) until the solution transformed into a dark violet gel. To study the influence of the sample packing prior to combustion synthesis, the gels were prepared in two different ways: one part of the gel as a loose packed layer (height ~ 5 mm) while the other was unaxially pressed (17 MPa) into a pellet (27 mm in diameter, height 15 mm, $\rho = 1.7$ g/cm^3). The samples were placed in an Al_2O_3 crucible and heated until they autoignited to give lanthanum chromite powders. The reaction period was measured. The reaction mixture compositions and preparation conditions are summarised in Table 1.

Table 1
Samples preparation conditions

Sample	c/n[a]	Sample packing prior combustion
A	0.18	loose packed layer
B	0.23	loose packed layer
C	0.28	loose packed layer
A1	0.18	pellet
B1	0.23	pellet
C1	0.28	pellet

[a] Citrate/nitrate ratio.

Table 2
Specific surface area and reaction period for all samples

Sample	Reaction period (s)	SSA (m^2/g)
A	6	11.74
B	8	12.09
C	60	12.52
A1	20	7.21
B1	34	8.13
C1	87	10.45

Samples were characterized by the X-ray powder diffraction technique using a Philips PW-1710 apparatus. Data were collected in the range from 5° to 65° 2Θ in steps of 0.03° for 1 s/step. TG analysis was performed on a NETZSCH STA 904C. A Perkin Elmer Sorptometer 212D was used to determine specific surface areas by the BET method. Samples were unaxially pressed at 70 and 300 MPa and analyzed by SEM (Scanning Electron Microscope, Jeol T300) and mercury porosimetry (Micromeritics 9310). Some samples were milled for 30 min in an agate ball mill; d_{50} was determined using an 850 CILAS ALCATEL granulometer. Shrinkage during sintering of some samples was measured by a LEITZ WETZLAR heating microscope. AC impedance measurements of sintered sam-

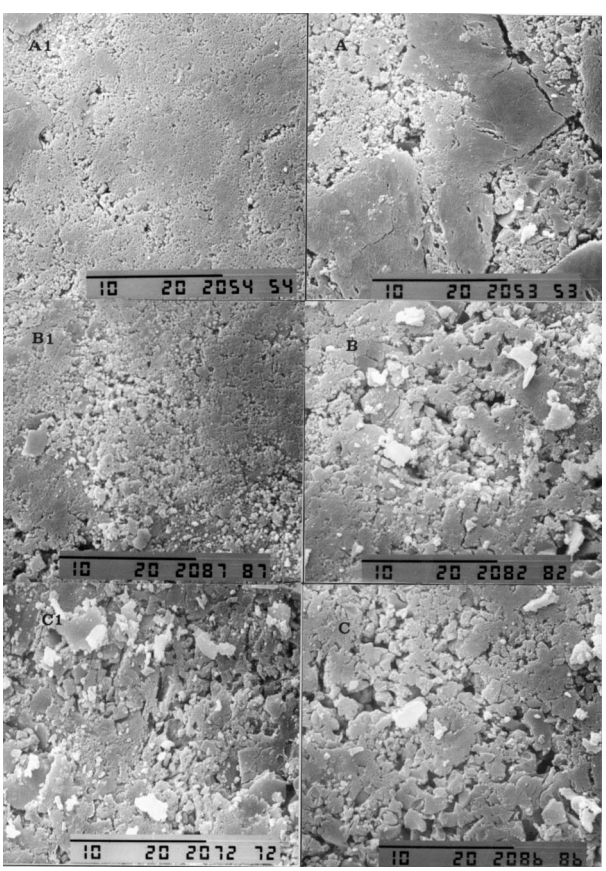

Fig. 1. SEM micrographs of all samples pressed at 300 MPa.

ples were carried out using an impedance analyzer (Hewlett Packard 4284A) over the frequency range from 20 Hz to 1 MHz for a temperature range from 30 to 1000°C in the atmosphere of static air.

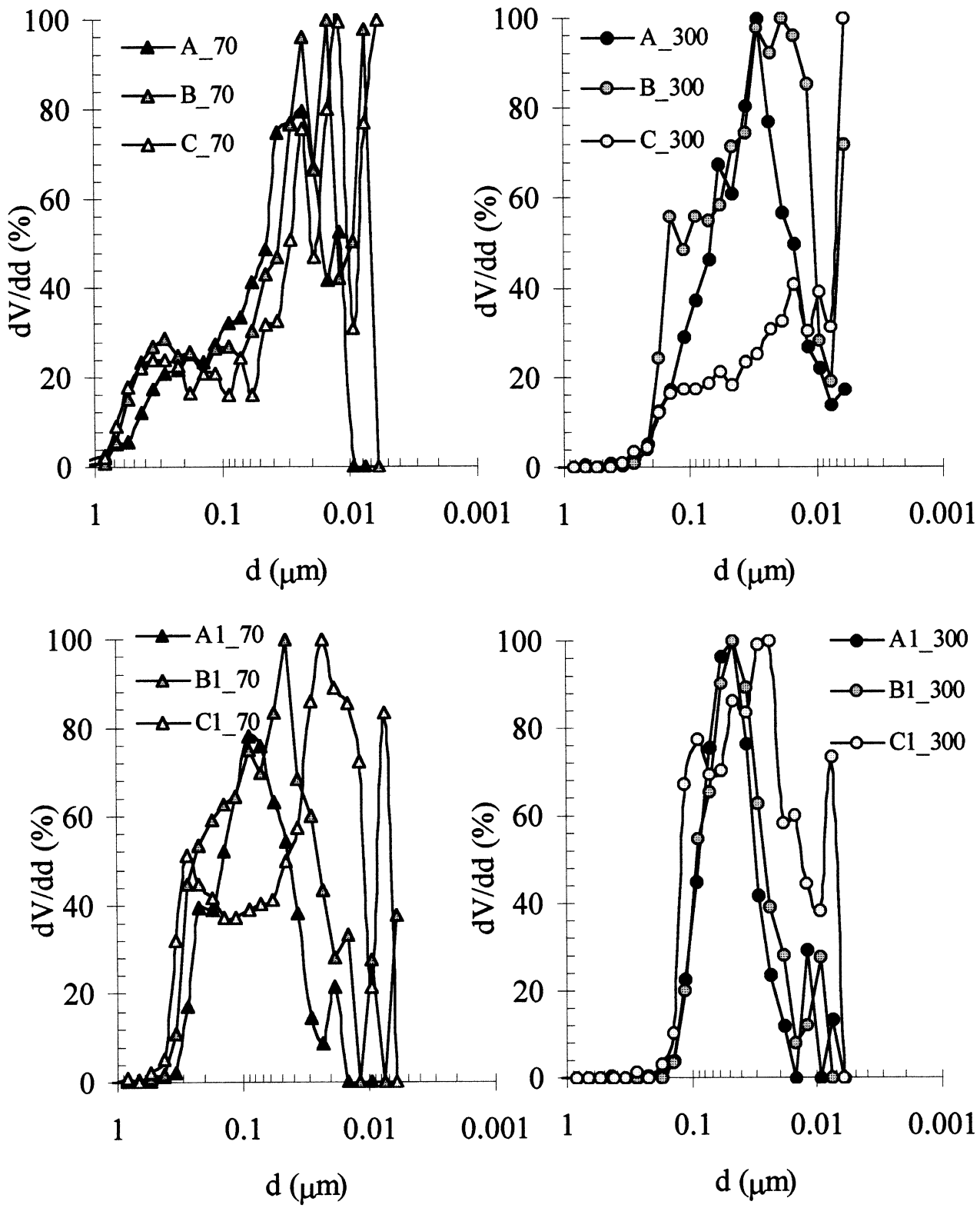

Fig. 2. Pore size frequency distribution of samples prepared in the layer form pressed at (a) 70 MPa and (b) 300 MPa, and in the pellet from pressed at (c) 70 MPa and (d) 300 MPa.

3. Results and discussion

Combustion velocities and specific surface areas (SSA) for samples are given in Table 2, showing that both increase with the increasing citrate content in the reaction mixture. Furthermore, visual observation revealed that mixtures with c/n ratios of 0.18 and 0.23 burned at higher temperatures than the mixture with c/n 0.28. The exact stoichiometric compositions cannot be calculated unless the compositions and proportions of all products are known (which was not determined in the present work). Considering the reaction scheme of Zhang and Stangle [9], compositions with c/n ratios of 0.23 and 0.18 are in the stoichiometric region, while the ratio 0.28 is considered fuel-rich. Their calculations of the stoichiometric fuel/oxidant ratio were based on the assumption that the oxidation state of the product species is not restricted to one value but may vary. For instance, the oxidation state of nitrogen in the reaction product may vary from 0 (as N_2) to 4+ (NO_2).

The combustion reaction time was longer (from 20 to 87 s) when burning proceeded in the pellet form while in the loose packed layer it lasted from 6 to 60 s. An explanation for this could be that the heat transfer in the pellet to the surface is retarded. The SSA of the pellet-formed powders increased from 7.21 to 10.45 m^2/g with increasing c/n ratio, while the SSA of the layer formed powders varied between 11.7 and 12.5 and was not markedly influenced by the citrate–nitrate ratio. During combustion, samples with higher c/n ratios liberate a lower amount gas, which diminishes the coarsening of the reaction products, resulting in a higher surface area. The effect of escaping gas is more pronounced in pellets than in loose powder.

Scanning electron micrographs of all samples pressed at 300 MPa are given in Fig. 1 showing that they are composed of particles from 50 to 150 nm in size. Particles are bound into agglomerates of different sizes and shapes. Samples prepared in a loose packed layer shows a considerable difference from those prepared in pellet form.

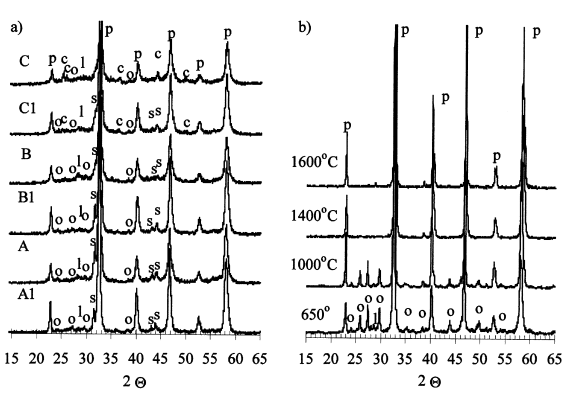

Fig. 3. X-ray diffraction patterns of (a) all samples, (b) sample A1 after calcination at different temperatures.

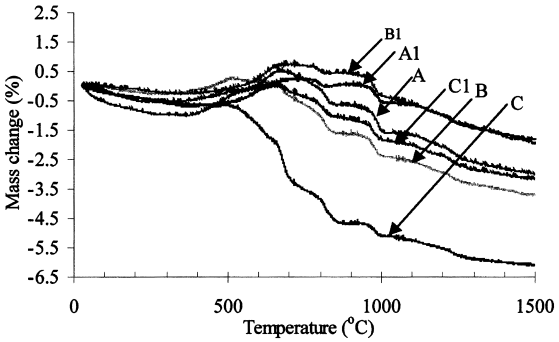

Fig. 4. TG curves of all samples.

Powder morphology depends on both the reaction mixture form and the citrate–nitrate ratio. Sample A is composed of dense agglomerates and less dense regions, while samples B and C possess large voids in the green structure. Mixtures A and B react very fast and samples were ejected due to temperature gradients in the sample. The reason for the inhomogeneous structure of loose powders may be due to temperature gradients during synthesis in sample A and a lower degree of conversion in samples B and C. The porous structure of samples C and C1 prepared from a fuel-rich reaction mixture is due to the lower combustion temperature and higher volume of escaping gas. As compared with other compositions, compositions A1 and B1 exhibit considerably less porous structures and more homogeneous particle arrangements.

The nature of the agglomerates prepared under various processing conditions was examined by evaluating the porosity of compacts pressed at 70 and 300 MPa. The pore size distributions of samples pressed at 70 and 300 MPa are shown in Fig. 2. Samples prepared in the layer form had pores from 1 to 0.006 μm when pressed at 70 MPa (Fig. 2a), while after pressing at 300 MPa (Fig. 2b) the size of the pores ranged from 0.4 to 0.006 μm (0.006 μm was the detection limit of our apparatus). Although the proportion of the larger pores from 1 to 0.1 μm in size decreased with increasing pressure, the pore size interval remained wide with pores from 0.4 to 0.006 μm in size. Samples prepared in the pellet form pressed at 70 and 300 MPa had pore size intervals from 0.7 to 0.006 μm and from 0.2 to 0.006 μm, respectively (Fig. 2c and d). Pores in sample C1 pressed at 70 MPa could be divided into larger pores from 0.7 to 0.06 μm and smaller ones from 0.06 to 0.006 μm in size. When pressing sample C1 at the higher pressure of 300 MPa the amount of larger pores was reduced; however, the pore size interval remained wider with pore diameters from 0.2 to 0.006 μm. Comparison of samples A1 and B1 to the others shows a much narrower pore size distribution with most pores between 0.2 and 0.02 μm. Homogeneous porosity in samples A1 and B1 indicates the weak nature of the agglomerates, allowing agglomerate breaking and rearrangement during pressing [10].

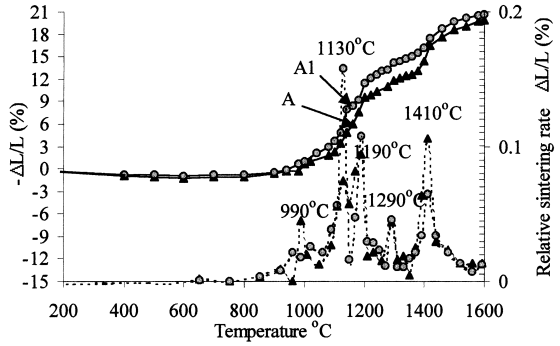

Fig. 5. Relative linear shrinkage and relative rate of sintering versus temperature of samples A1 and A milled for 30 min and pressed at 70 MPa.

Phase compositions of all as-prepared samples were determined by X-ray diffraction. The XRD curves (Fig. 3a) of as-prepared samples suggest that the samples were not well crystallized, being mainly composed of the perovskite crystalline phase. In all samples secondary $SrCrO_4$ and La_2CrO_6 phases were found. Regarding these secondary phases, samples A, A1 and B1 contained one the of so-called Ruddlesden Popper phases, Sr_2CrO_4. Traces of this phase were found in other samples. A strontium rich phase with Cr^{4+} was formed in an oxygen deficient atmosphere [11]. Oxygen access may have been partly hindered due to the form of the sample before combustion when synthesis was performed as a pellet and due to rapid gas evolution. In samples B, C and C1, $SrCO_3$ was detected. The presence of strontium carbonate could be due to the short reaction time (sample B) as well as the excess of citric acid (C and C1). After the calcination of sample A1 (Fig. 3b) at 650°C, the sample was well crystallized and its diffraction pattern corresponded to orthorhombic symmetry. Secondary phases $SrCrO_4$ and La_2CrO_6 were found. After calcination at 1000°C, the only secondary phase present was $SrCrO_4$, while after heat treatment at 1400°C chromite phase and traces of $SrCrO_4$ were detected. The multiple diffraction peaks after heating at 1600°C become stronger indicating the disordered nature of the LSC [12].

As expected from their variable phase composition, the thermal behaviour of the samples is considerably different depending on the citrate–nitrate ratio and sample form prior to combustion (Fig. 4). Total mass loss increases with increasing c/n ratio. Minor mass losses (from 1.8 to 3.2%) were observed during thermal analysis in case of pelletised samples, while mass loss from 3 to 6.2% for the layer prepared samples indicates a lower degree of conversion of these samples. The lower combustion temperature and shorter time at reaction temperature for sample C was confirmed optically by a noticeable mass loss (2.9%) in the temperature region from 400 to 700°C due to removal of organic residues. In contrast, samples A, A1 and B1 gained mass in the temperature range from 365 to 700°C, probably due to oxidation of Sr_2CrO_4 ($Sr_2CrO_4 + O_2 \rightarrow SrCrO_4 + SrO$) as shown elsewhere (to be published). Weight loss above 1000°C indicates decomposition of secondary phases such as $SrCO_3$ and La_2CrO_6.

Table 3
Densities, relative mass and dimensional changes for samples A and A1 sintered at 1600°C 10 h

Sample	ρ_g	ρ_s	$\rho_{hex\ powder}$	$\rho_{s(relative)}$ (%)	Δm (%)	$\Delta\phi$ (%)	Δh (%)
A1	3.28	6.09	6.34	96	1.63	19.08	18.97
A	3.18	5.8	6.34	91	3.6	19.08	19.2

Table 4
Specific electrical conductivities for samples A and A1 sintered 1600°C for 10 h

Sample	Specific electrical conductivity (S/cm)	
	30°C	1000°C
A1	0.016	17.6
A	0.013	7.4

Sintering curves of samples A and A1 (milled for 30 min in an agate mill, $d_{50} \sim 1.2$ μm, unaxially pressed at 70 MPa) are shown in Fig. 5. The green density of A and A1 compacts was 2.8 g/cm^3. From Fig. 5, it is evident that shrinkage for both samples occurred in several steps. The shrinking process initiated at 800°C, and was followed by several shrinkage maxima at 990°C, 1130°C, 1190°C, 1290°C and 1410°C in both samples due to the presence of secondary phases (La_2CrO_6 and $SrCrO_4$). The inflection at 1290°C is associated with liquid phase formation. Although the presence of $SrCrO_4$ and subsequent melting is not as effective as that in yttrium chromite substituted with calcium, it still partly enhances densification [13]. According to the literature, the effectiveness of the lanthanum-rich phase La_2CrO_6 as a sintering aid can be attributed to the resulting increase in the ratio A/B in the ABO_3 structure (La + Sr = A and B = Cr) and changes in the unit cell density [6]. However, sample A1 with a relative linear shrinkage of 11.4% densified faster than sample A with a

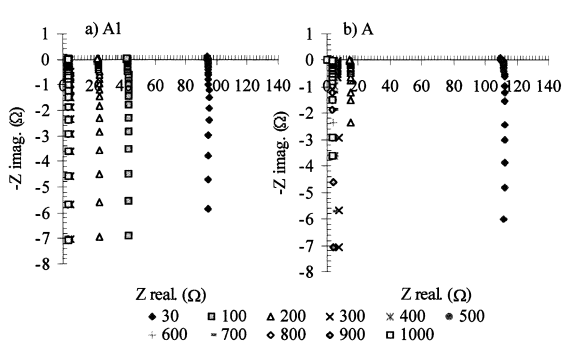

Fig. 6. Impedance spectra of samples A1 and A after sintering at 1600°C taken in static air at different temperatures.

relative linear shrinkage of 9.5% at 1200°C. Obviously, powder homogeneity and particles packing cause faster sintering of sample A1. The sintering behaviour difference was confirmed by sintering of samples A1 and A at 1600°C for 10 h (Table 3). The relative sintering density was calculated from the density of the reacted powder determined by hexane picnometry. The higher density of sample A1 (96% TD) than sample A reflects the advantage of combustion synthesis in the pellet form.

As expected from the different sintering behaviour, the electrical conductivities of samples A1 and A are different (Table 4). The two samples have similar conductivities at 30°C while at 1000°C sample A prepared in the layer form exhibits a significantly lower conductivity than sample A1 prepared in pellet form. According to the literature, in samples with higher Sr content (from 10 to 20 at.% Sr) electrical conductivity is increased exclusively due to the additional effect of densification [14]. According to the impedance measurements shown in Fig. 6a and b, both samples possess good conductivities. No capacitive elements were observed when varying the frequency through the chosen range. The electrical resistivity of both samples decreases with increasing temperature, a behaviour typical of semiconductors. The electrical conductivity of sample A1 is in good agreement with a reported value of 14.3 S/cm [15].

4. Conclusions

Fuel/oxidant ratio and reaction mixture form prior to combustion (loose powder layer or compacted pellet) influence powder properties of samples after combustion. Temperature gradients during synthesis in samples prepared in the layer form result in less homogeneous porosity and a lower degree of conversion. The appropriate c/n ratio was found to be 0.18 to 0.23, while the combustion should be performed in the pellet form where mass losses after combustion do not exceed 2% and so-called weak agglomerates are formed. The relative sintered density and specific electrical conductivity of compacts sintered at 1600°C from samples prepared in the pellet form were 96% and 17.6 S/cm, values which are markedly higher than in the case of samples prepared in the layer form.

References

[1] M.R. Morelli, R.J. Brook, Ceram. Trans. 51 (1995) 81–85.
[2] N. Sakai, H. Yokohava, T. Kawada, M. Dokiya, I. Kojima, T. Iwata, J. Mater. Sci. 25 (1990) 4531–4534.
[3] R.A. Roosen, H. Hausner, in: P. Vincenzini (Ed.), The Influence of Processing Conditions on the Sintering Behaviour of Coprecipitated Calcia-Stabilized Zirconia Powders, Mater. Sci. Monogr. 16, Ceramic Powders, Elsevier, Amsterdam, 1983, pp. 773–782.
[4] K. Vidyasagar, J. Gopalakrishnan, R. Rao, Inorg. Chem. 23 (1984) 1206–1210.
[5] S. Bilger, G. Blass, R. Forthmann, J. Eur. Ceram. Soc. 17 (1997) 1027–1031.
[6] M.R. De Guire, S.E. Dorris, R.B. Poeppel, S. Morissette, U. Balacandran, J. Mater. Res. 8 (1993) 2327–2335.
[7] S. Roy, A. Das Sharma, S.N. Roy, H.S. Maiti, J. Mater. Res. 8 (1993) 2761–2766.
[8] Ph. Courty, H. Ajot, Ch. Marcilly, B. Delmon, Powder Technol. 7 (1973) 21–38.
[9] Y. Zhang, G.C. Stangle, J. Mater. Res. 9 (1994) 1997–2004.
[10] R. Pampuch, K. Haberko, in: P. Vincenzini (Ed.), Agglomerates in Ceramics Micropowders and Their Behaviour on Cold Pressing and Sintering, Mater. Sci. Monogr. 16, Ceramic Powders, Elsevier, Amsterdam, 1983, pp. 623–634.
[11] H. Yokokawa, N. Sakai, T. Kawada, M. Dokiya, J. Electrochem. Soc. 138 (1991) 1018–1027.
[12] A.M. Glazer, Acta Crystallogr. B28 (1972) 3384–3392.
[13] L.A. Chick, J.L. Bates, G.D. Maupin, Air Sintering Mechanisms of Chromites, Proceedings of the 2nd International Symposium on SOFC, Athens, 1991, pp. 621–628.
[14] P.H. Duvigneaud, P. Pilate, F. Cambier, J. Euro. Ceram. Soc. 14 (1994) 359–367.
[15] N.Q. Minh, J. Am. Ceram. Soc. 76 (1993) 563–588.
[16] A. Furusaki, H. Konno, R. Furuichi, J. Mater. Sci. 30 (1995) 2829–2834.